Supplementary Information (SI) for Physical Chemistry Chemical Physics.

Supporting Information: Finite-Field Cholesky Decomposed Coupled-Cluster Techniques (ff-CD-CC): Theory and Application to Pressure Broadening of Mg by a He Atmosphere and a Strong Magnetic Field

Simon Blaschke,[*,†,‡] Marios-Petros Kitsaras,[*,¶] and Stella Stopkowicz[*,¶,§]

†*Department Chemie, Johannes Gutenberg-Universität Mainz, Duesbergweg 10-14, D-55128 Mainz, Germany*

‡*Fachrichtung Chemie, Universität des Saarlandes, Campus B2.2, D-66123 Saarbrücken, Germany*

¶*Fachrichtung Chemie, Universität des Saarlandes, D-66123 Saarbrücken, Germany*

§*Hylleraas Centre for Quantum Molecular Sciences, Department of Chemistry, University of Oslo, P.O. Box 1033, N-0315 Oslo, Norway*

E-mail: siblasch@uni-mainz.de; marios.kitsaras@uni-saarland.de; stella.stopkowicz@uni-saarland.de

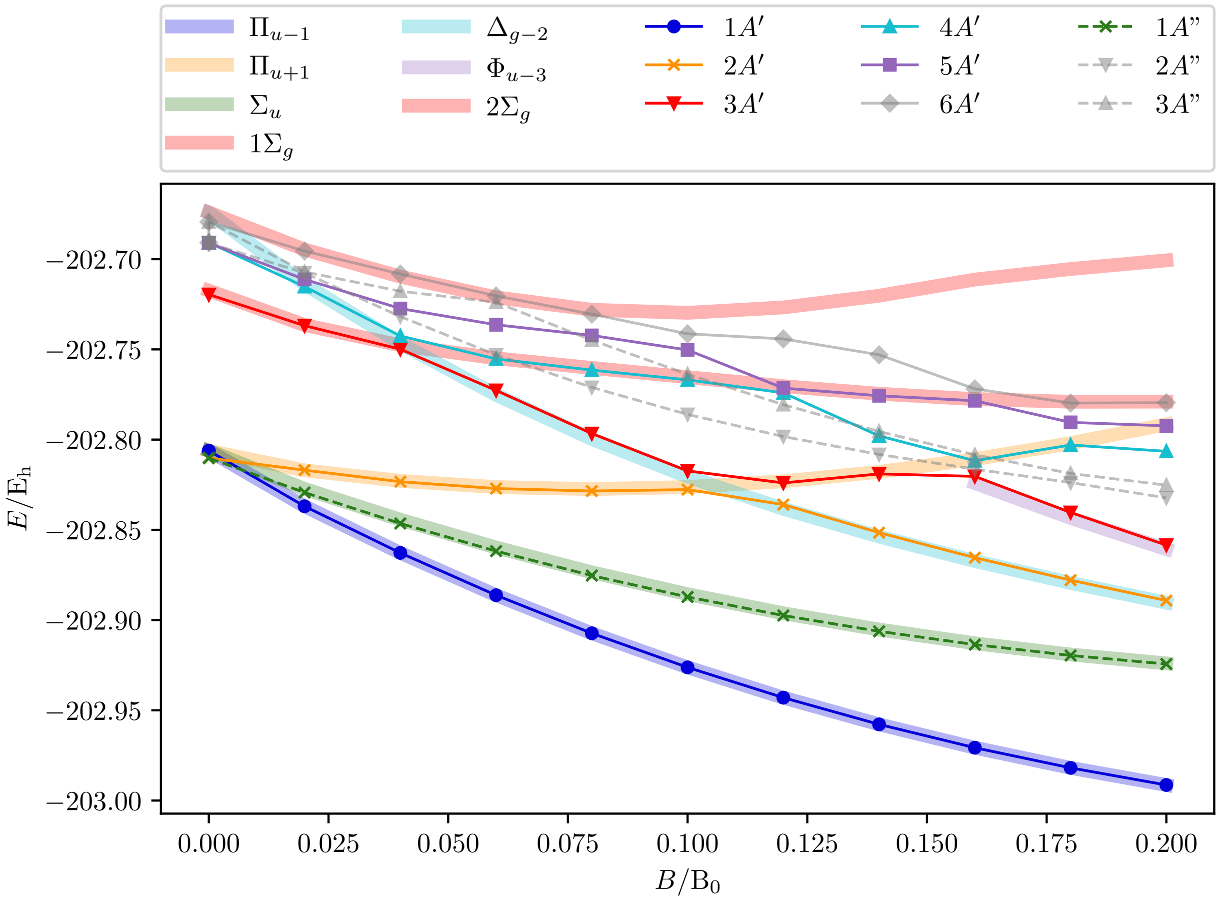

Figure S1: Depiction of the ground and excited states of MgHe in a perpendicular magnetic field (C_s). As a guideline of the evolution of the states in the isolated Mg atom ($SO(3)$) the respective states are shown as broad lines. Note that they were shifted by the energy of the helium atom so that the ground state coincides.

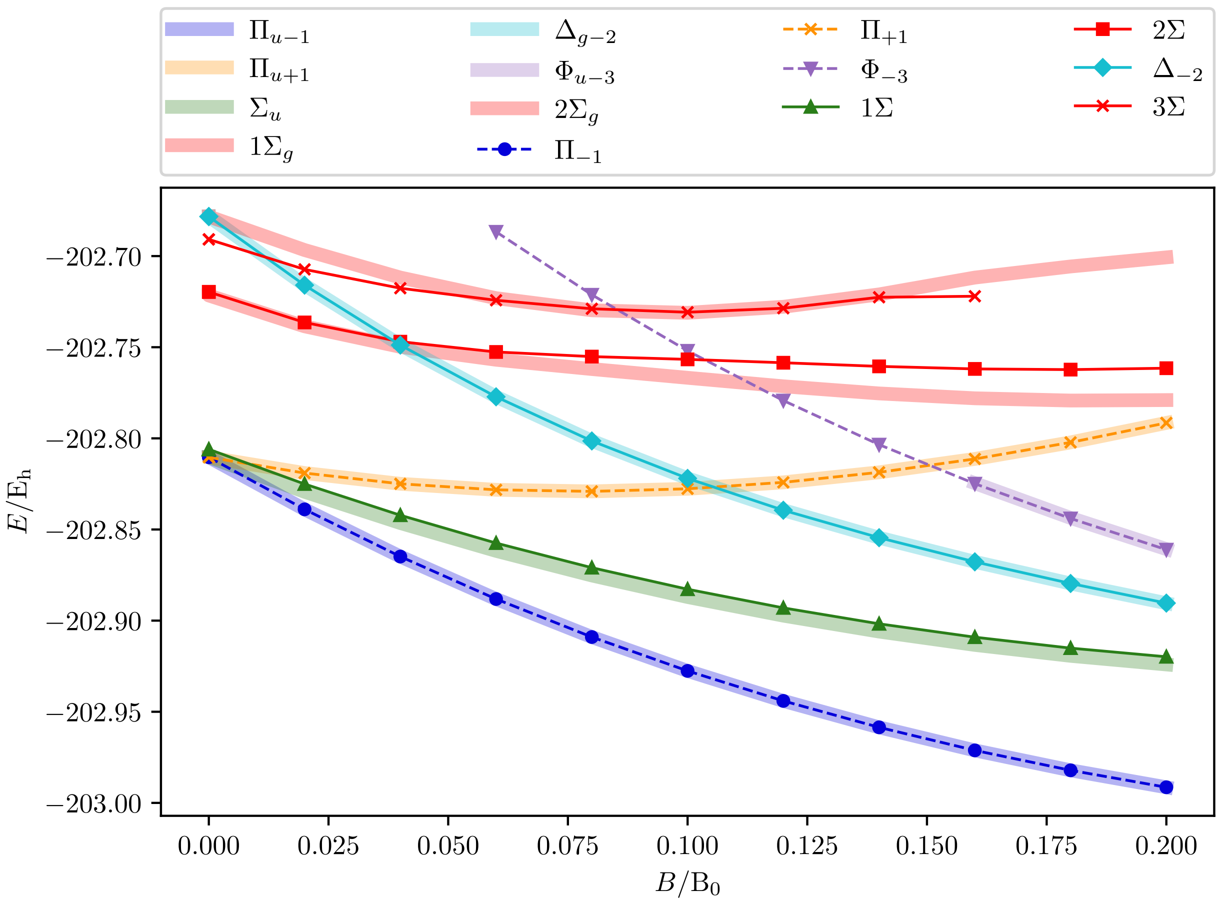

Figure S2: Depiction of the ground and excited states of MgHe in a parallel magnetic field (C_∞). As a guideline of the evolution of the states in the isolated Mg atom ($SO(3)$) the respective states are shown as broad lines. Note that they were shifted by the energy of the helium atom so that the ground state coincides.

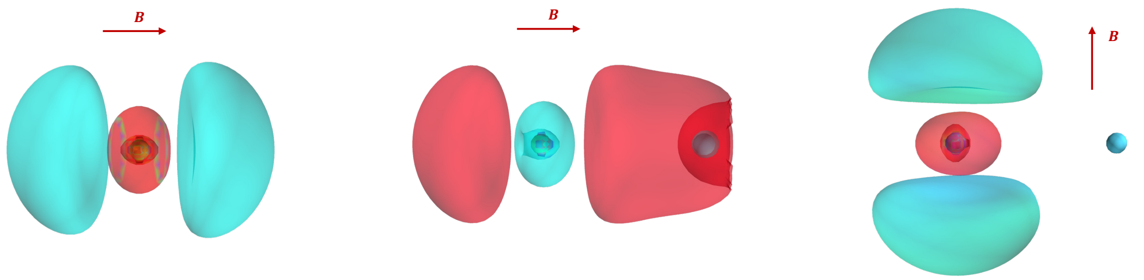

Figure S3: Depiction of the HOMO (4s in the field-free case) of the final state for the ^3P to ^3S transition of the Mg triplet atom (left) in a magnetic field and for MgHe with the magnetic field parallel (center) and perpendicular (right) to the bond axis. Calculated at B=0.1 B_0 as an isosurface plot of 0.015 a_0^{-3}.

Table S1: EOM-CCSD excitation energy E_{exc} of the MgHe dimer at 3.5 Å bond distance. The basis set on Mg was chosen to be unc-aug-cc-pCVQZ while the basis on He was varied. The difference in the transition wavelength $\Delta\lambda$ with respect to the d-aug-cc-pVQZ is given additionally.

Basis on He	$E_{\mathrm{exc}}/E_{\mathrm{h}}$	$\Delta E_{\mathrm{exc}}/E_{\mathrm{h}}$	$\Delta\lambda$/Å
unc-6-31G	$9.097\,78 \times 10^{-2}$	3.1×10^{-4}	16.95
unc-cc-pVDZ	$9.093\,17 \times 10^{-2}$	2.6×10^{-4}	14.41
unc-aug-cc-pVDZ	$9.073\,52 \times 10^{-2}$	6.4×10^{-5}	3.55
unc-aug-cc-pVTZ	$9.069\,67 \times 10^{-2}$	2.6×10^{-5}	1.42
unc-aug-cc-pVQZ	$9.068\,80 \times 10^{-2}$	1.7×10^{-5}	0.94
unc-d-aug-cc-pVQZ	$9.067\,11 \times 10^{-2}$	0.00	0.00

Table S2: Mean error of the ff-CD-HF energy, ff-CD-CCSD/CC2 correlation energy and the ff-CD-EOM-CCSD/CC2 excitation energy as a function of the Cholesky parameter δ. The convergence criteria for HF, CCSD as well as EOM were set to 10^{-7}.

δ	$\Delta E_{\mathrm{HF}}/E_{\mathrm{h}}$	$\Delta E_{\mathrm{CCSD}}/E_{\mathrm{h}}$	$\Delta E_{\mathrm{EOM-CCSD}}/E_{\mathrm{h}}$	$\Delta E_{\mathrm{CC2}}/E_{\mathrm{h}}$	$\Delta E_{\mathrm{EOM-CC2}}/E_{\mathrm{h}}$
1	3.7×10^{-2}	2.9×10^{-2}	2.1×10^{-2}	2.3×10^{-2}	1.2×10^{-2}
2	9.0×10^{-4}	2.5×10^{-4}	1.9×10^{-4}	5.2×10^{-4}	2.2×10^{-4}
3	1.8×10^{-5}	6.7×10^{-6}	6.3×10^{-6}	2.1×10^{-5}	5.8×10^{-6}
4	1.6×10^{-6}	2.9×10^{-7}	5.2×10^{-7}	9.5×10^{-7}	4.0×10^{-7}
5	6.4×10^{-7}	9.0×10^{-8}	6.5×10^{-8}	1.8×10^{-7}	5.7×10^{-8}
6	4.7×10^{-8}	8.6×10^{-9}	1.4×10^{-8}	1.6×10^{-8}	1.2×10^{-8}
7	1.3×10^{-8}	3.5×10^{-9}	2.0×10^{-9}	4.2×10^{-9}	3.4×10^{-9}
8	9.3×10^{-10}	2.6×10^{-9}	6.4×10^{-10}	3.0×10^{-9}	2.5×10^{-9}
9	5.3×10^{-11}	2.6×10^{-9}	3.6×10^{-10}	3.0×10^{-9}	2.3×10^{-9}
10	0.0	2.6×10^{-9}	3.4×10^{-10}	3.0×10^{-9}	2.3×10^{-9}

Table S3: The transition wavelength λ ($^3\Pi \rightarrow ^3\Sigma^+$) as well as the total initial state energy E_{tot} as a function of the Mg-He distance R. Calculated with CD-CCSD ($\delta = 5$) using the unc-aug-cc-pCVQZ basis for Mg and the unc-aug-cc-pVDZ basis for He.

R/Å	λ/Å	$E_{\mathrm{tot}}/E_{\mathrm{h}}$
2.00	5196.55	-202.803197
2.50	5104.26	-202.808283
3.00	5040.01	-202.809948
3.50	5024.26	-202.810382
4.00	5034.37	-202.810435
4.50	5054.82	-202.810408
5.00	5076.51	-202.810375
5.50	5094.98	-202.810353
6.00	5108.79	-202.810341
6.50	5118.24	-202.810334
7.00	5124.27	-202.810330
7.50	5127.92	-202.810328
8.00	5130.04	-202.810327
8.50	5131.22	-202.810326
9.00	5131.85	-202.810325
9.50	5132.17	-202.810325
10.00	5132.32	-202.810325
10.50	5132.38	-202.810325
11.00	5132.40	-202.810324
11.50	5132.40	-202.810324
12.00	5132.40	-202.810324
12.50	5132.39	-202.810324
13.00	5132.38	-202.810324
13.50	5132.38	-202.810324
14.00	5132.37	-202.810324
14.50	5132.37	-202.810324
15.00	5132.37	-202.810324

Table S4: Total energy E_{tot} of the initial and first two final states of the MgHe triplet dimer without an external magnetic field and within an finite magnetic field of $0.05\,\text{B}_0$ oriented parallel and perpendicular with respect to the Mg-He axis. The calculations were performed at the unc-aug-cc-pVTZ/CC3 level of theory.

	$B = 0$		
R/Å	$E_{\text{tot}}(^3\Sigma^+)/E_\text{h}$	$E_{\text{tot}}(^3\Pi_{-1})/E_\text{h}$	$E_{\text{tot}}(^3\Pi_{+1})/E_\text{h}$
3.0	-202.621464	-202.631647	-202.631647
3.5	-202.627884	-202.632085	-202.632085
4.0	-202.630494	-202.632140	-202.632140
4.5	-202.631507	-202.632121	-202.632121
5.0	-202.631881	-202.632097	-202.632097
5.5	-202.632011	-202.632079	-202.632079
6.0	-202.632052	-202.632068	-202.632068
6.5	-202.632062	-202.632062	-202.632062
7.0	-202.632064	-202.632058	-202.632058
7.5	-202.632063	-202.632056	-202.632056
8.0	-202.632061	-202.632055	-202.632055
	$B \parallel$		
R/Å	$E_{\text{tot}}(^3\Sigma)/E_\text{h}$	$E_{\text{tot}}(^3\Pi_{-1})/E_\text{h}$	$E_{\text{tot}}(^3\Pi_{+1})/E_\text{h}$
3.0	-202.665333	-202.698023	-202.648026
3.5	-202.671842	-202.698480	-202.648483
4.0	-202.674479	-202.698543	-202.648545
4.5	-202.675498	-202.698527	-202.648529
5.0	-202.675872	-202.698505	-202.648507
5.5	-202.676001	-202.698488	-202.648490
6.0	-202.676041	-202.698477	-202.648479
6.5	-202.676052	-202.698471	-202.648473
7.0	-202.676053	-202.698467	-202.648469
7.5	-202.676052	-202.698465	-202.648467
8.0	-202.676050	-202.698464	-202.648466
	$B \perp$		
R/Å	$E_{\text{tot}}(^3A')/E_\text{h}$	$E_{\text{tot}}(^3A'')/E_\text{h}$	$E_{\text{tot}}(^3A')/E_\text{h}$
3.00	-202.693170	-202.675735	-202.644368
3.50	-202.696482	-202.676114	-202.647151
4.00	-202.697802	-202.676144	-202.648083
4.50	-202.698275	-202.676116	-202.648380
5.00	-202.698427	-202.676089	-
5.50	-202.698467	-202.676071	-202.648481
6.00	-202.698473	-202.676061	-202.648479
6.50	-202.698471	-202.676055	-202.648474
7.00	-202.698468	-202.676051	-202.648470
7.50	-202.698466	-202.676050	-202.648468
8.00	-202.698464	-202.676048	-202.648466

Table S5: The counterpoise corrected CCSD interaction energy of the initial state of the MgHe triplet dimer as a function of the external magnetic field strength in a parallel orientation respectively. The calculations were performed using the unc-aug-cc-pCVQZ basis for Mg and the unc-aug-cc-pVDZ basis for He.

R/Å	$B = 0.0$ B$_0$ $E_{\text{int}}/E_{\text{h}}$	$B = 0.05$ B$_0$ $E_{\text{int}}/E_{\text{h}}$	$B = 0.10$ B$_0$ $E_{\text{int}}/E_{\text{h}}$	$B = 0.15$ B$_0$ $E_{\text{int}}/E_{\text{h}}$	$B = 0.20$ B$_0$ $E_{\text{int}}/E_{\text{h}}$
3.0	5.300×10^{-4}	5.508×10^{-4}	5.960×10^{-4}	6.562×10^{-4}	7.271×10^{-4}
3.5	2.016×10^{-5}	2.891×10^{-5}	4.669×10^{-5}	6.869×10^{-5}	9.371×10^{-5}
3.6	-1.458×10^{-5}	-7.147×10^{-6}	7.775×10^{-6}	2.591×10^{-5}	4.630×10^{-5}
3.7	-3.782×10^{-5}	-3.148×10^{-5}	-1.889×10^{-5}	-3.865×10^{-6}	1.279×10^{-5}
3.8	-5.249×10^{-5}	-4.705×10^{-5}	-3.637×10^{-5}	-2.387×10^{-5}	-1.023×10^{-5}
3.9	-6.087×10^{-5}	-5.618×10^{-5}	-4.708×10^{-5}	-3.662×10^{-5}	-2.541×10^{-5}
4.0	-6.473×10^{-5}	-6.068×10^{-5}	-5.288×10^{-5}	-4.409×10^{-5}	-3.484×10^{-5}
4.1	-6.543×10^{-5}	-6.191×10^{-5}	-5.520×10^{-5}	-4.777×10^{-5}	-4.012×10^{-5}
4.2	-6.399×10^{-5}	-6.092×10^{-5}	-5.512×10^{-5}	-4.881×10^{-5}	-4.245×10^{-5}
4.3	-6.116×10^{-5}	-5.847×10^{-5}	-5.344×10^{-5}	-4.805×10^{-5}	-4.274×10^{-5}
4.4	-5.748×10^{-5}	-5.513×10^{-5}	-5.075×10^{-5}	-4.613×10^{-5}	-4.168×10^{-5}
4.5	-5.337×10^{-5}	-5.130×10^{-5}	-4.747×10^{-5}	-4.350×10^{-5}	-3.975×10^{-5}
4.6	-4.909×10^{-5}	-4.727×10^{-5}	-4.391×10^{-5}	-4.049×10^{-5}	-3.730×10^{-5}
4.7	-4.484×10^{-5}	-4.323×10^{-5}	-4.028×10^{-5}	-3.731×10^{-5}	-3.460×10^{-5}
4.8	-4.074×10^{-5}	-3.931×10^{-5}	-3.672×10^{-5}	-3.414×10^{-5}	-3.182×10^{-5}
4.9	-3.687×10^{-5}	-3.561×10^{-5}	-3.332×10^{-5}	-3.107×10^{-5}	-2.907×10^{-5}
5.0	-3.327×10^{-5}	-3.215×10^{-5}	-3.014×10^{-5}	-2.816×10^{-5}	-2.643×10^{-5}
5.5	-1.956×10^{-5}	-1.893×10^{-5}	-1.782×10^{-5}	-1.677×10^{-5}	-1.587×10^{-5}
6.0	-1.159×10^{-5}	-1.122×10^{-5}	-1.059×10^{-5}	-9.987×10^{-6}	-9.475×10^{-6}
6.5	-7.070×10^{-6}	-6.846×10^{-6}	-6.466×10^{-6}	-6.103×10^{-6}	-5.792×10^{-6}
7.0	-4.465×10^{-6}	-4.323×10^{-6}	-4.082×10^{-6}	-3.851×10^{-6}	-3.652×10^{-6}
7.5	-2.916×10^{-6}	-2.822×10^{-6}	-2.663×10^{-6}	-2.509×10^{-6}	-2.375×10^{-6}
8.0	-1.962×10^{-6}	-1.897×10^{-6}	-1.789×10^{-6}	-1.682×10^{-6}	-1.590×10^{-6}

Table S6: The counterpoise corrected CCSD interaction energy of the initial state of the MgHe triplet dimer as a function of the external magnetic field strength in a perpendicular orientation respectively. The calculations were performed using the unc-aug-cc-pCVQZ basis for Mg and the unc-aug-cc-pVDZ basis for He.

R/Å	$B = 0.0$ B$_0$ $E_{\mathrm{int}}/E_{\mathrm{h}}$	$B = 0.05$ B$_0$ $E_{\mathrm{int}}/E_{\mathrm{h}}$	$B = 0.10$ B$_0$ $E_{\mathrm{int}}/E_{\mathrm{h}}$	$B = 0.15$ B$_0$ $E_{\mathrm{int}}/E_{\mathrm{h}}$	$B = 0.20$ B$_0$ $E_{\mathrm{int}}/E_{\mathrm{h}}$
3.0	5.300×10^{-4}	5.421×10^{-3}	4.623×10^{-3}	3.078×10^{-3}	1.588×10^{-3}
3.5	2.016×10^{-5}	2.048×10^{-3}	1.424×10^{-3}	6.667×10^{-4}	1.132×10^{-4}
3.6	-1.458×10^{-5}	1.664×10^{-3}	1.100×10^{-3}	4.606×10^{-4}	2.193×10^{-5}
3.7	-3.782×10^{-5}	1.347×10^{-3}	8.423×10^{-4}	3.067×10^{-4}	-3.680×10^{-5}
3.8	-5.249×10^{-5}	1.085×10^{-3}	6.384×10^{-4}	1.936×10^{-4}	-7.215×10^{-5}
3.9	-6.087×10^{-5}	8.712×10^{-4}	4.782×10^{-4}	1.118×10^{-4}	-9.112×10^{-5}
4.0	-6.473×10^{-5}	6.962×10^{-4}	3.533×10^{-4}	5.383×10^{-5}	-9.894×10^{-5}
4.1	-6.543×10^{-5}	5.538×10^{-4}	2.566×10^{-4}	1.384×10^{-5}	-9.947×10^{-5}
4.2	-6.399×10^{-5}	4.383×10^{-4}	1.823×10^{-4}	-1.284×10^{-5}	-9.547×10^{-5}
4.3	-6.116×10^{-5}	3.449×10^{-4}	1.259×10^{-4}	-2.980×10^{-5}	-8.890×10^{-5}
4.4	-5.748×10^{-5}	2.697×10^{-4}	8.331×10^{-5}	-3.978×10^{-5}	-8.107×10^{-5}
4.5	-5.337×10^{-5}	2.094×10^{-4}	5.163×10^{-5}	-4.484×10^{-5}	-7.285×10^{-5}
4.6	-4.909×10^{-5}	1.612×10^{-4}	2.838×10^{-5}	-4.655×10^{-5}	-6.480×10^{-5}
4.7	-4.484×10^{-5}	1.228×10^{-4}	1.159×10^{-5}	-4.602×10^{-5}	-5.722×10^{-5}
4.8	-4.074×10^{-5}	9.245×10^{-5}	-2.602×10^{-7}	-4.408×10^{-5}	-5.029×10^{-5}
4.9	-3.687×10^{-5}	6.849×10^{-5}	-8.386×10^{-6}	-4.131×10^{-5}	-4.407×10^{-5}
5.0	-3.327×10^{-5}	4.970×10^{-5}	-1.373×10^{-5}	-3.813×10^{-5}	-3.857×10^{-5}
5.1	-	3.505×10^{-5}	-1.701×10^{-5}	-3.479×10^{-5}	-3.374×10^{-5}
5.2	-	2.372×10^{-5}	-1.880×10^{-5}	-3.150×10^{-5}	-2.954×10^{-5}
5.3	-	1.503×10^{-5}	-1.953×10^{-5}	-2.835×10^{-5}	-2.589×10^{-5}
5.4	-	8.431×10^{-6}	-1.950×10^{-5}	-2.541×10^{-5}	-2.274×10^{-5}
5.5	-1.956×10^{-5}	3.478×10^{-6}	-1.897×10^{-5}	-2.272×10^{-5}	-2.001×10^{-5}
5.6	-	-1.791×10^{-7}	-1.811×10^{-5}	-2.028×10^{-5}	-1.764×10^{-5}
5.7	-	-2.825×10^{-6}	-1.706×10^{-5}	-1.809×10^{-5}	-1.560×10^{-5}
5.8	-	-4.687×10^{-6}	-1.591×10^{-5}	-1.613×10^{-5}	-1.383×10^{-5}
5.9	-	-5.944×10^{-6}	-1.472×10^{-5}	-1.440×10^{-5}	-1.229×10^{-5}
6.0	-1.159×10^{-5}	-6.740×10^{-6}	-1.355×10^{-5}	-1.286×10^{-5}	-1.095×10^{-5}
6.1	-	-7.188×10^{-6}	-1.241×10^{-5}	-1.150×10^{-5}	-9.781×10^{-6}
6.2	-	-7.376×10^{-6}	-1.134×10^{-5}	-1.030×10^{-5}	-8.757×10^{-6}
6.3	-	-7.373×10^{-6}	-1.033×10^{-5}	-9.239×10^{-6}	-7.859×10^{-6}
6.4	-	-7.234×10^{-6}	-9.399×10^{-6}	-8.302×10^{-6}	-7.068×10^{-6}
6.5	-7.070×10^{-6}	-6.999×10^{-6}	-8.544×10^{-6}	-7.474×10^{-6}	-6.370×10^{-6}
7.0	-4.465×10^{-6}	-5.271×10^{-6}	-5.307×10^{-6}	-4.538×10^{-6}	-3.897×10^{-6}
7.5	-2.916×10^{-6}	-3.640×10^{-6}	-3.364×10^{-6}	-2.873×10^{-6}	-2.482×10^{-6}
8.0	-1.962×10^{-6}	-2.464×10^{-6}	-2.196×10^{-6}	-1.884×10^{-6}	-1.635×10^{-6}

Table S7: Transition wavelength λ of the three former P-states as a function of the magnetic field strength B. Three cases are distinguished. The isolated Mg atom is used as a reference ($C_{\infty h}$, solid) and is compared with the MgHe triplet dimer at the equilibrium distance in the parallel (C_∞) or perpendicular (C_s) magnetic field. Calculated with CD-CCSD ($\delta = 5$) using the unc-aug-cc-pCVQZ basis for Mg and the unc-aug-cc-pVDZ basis for He.

Mg atom			
B/ B_0	$\lambda(^3\Pi_u)$/Å	$\lambda(^3\Sigma_u)$/Å	$\lambda(^3\Pi_u)$/Å
0.00	5132.4	5132.4	5132.4
0.02	4539.7	5021.7	5662.3
0.04	3962.0	4716.5	6065.8
0.05	3703.6	4532.4	6229.5
0.06	3472.9	4348.4	6388.4
0.08	3100.6	4025.6	6791.9
0.10	2835.0	3790.7	7485.5
0.12	2641.3	3623.3	8651.0
0.14	2488.6	3489.5	10532.6
0.15	2422.0	3428.5	11895.3
0.16	2360.0	3369.5	13704.1
0.18	2247.2	3254.9	19852.1
0.20	2146.1	3143.1	36412.4
MgHe $B \perp$			
B/ B_0	$\lambda(^3A')$/Å	$\lambda(^3A'')$/Å	$\lambda(^3A')$/Å
0.00	5037.0	5116.8	5037.0
0.05	3674.1	4459.2	6126.9
0.10	2841.3	3790.4	7488.6
0.15	2424.9	3431.1	11886.1
0.20	2148.0	3146.9	36562.7
MgHe $B \parallel$			
B/ B_0	$\lambda(^3\Pi_{-1})$/Å	$\lambda(^3\Sigma)$/Å	$\lambda(^3\Pi_{+1})$/Å
0.00	5037.0	5116.8	5037.0
0.05	3620.3	4471.0	5997.3
0.10	2713.1	3616.1	6691.8
0.15	2299.1	3217.7	9421.4
0.20	2043.9	2952.8	19693.7

Table S8: Shift in the excitation energies ΔE_{exc} induced by the helium atom for the three former P-states of the MgHe triplet dimer at the equilibrium distance in a parallel (C_∞) or perpendicular (C_s) magnetic field compared to the isolated Mg atom. For the absolute excitation energies also see tab. S7.

	MgHe $B \perp$			MgHe $B \parallel$		
	$^3A'$	$^3A''$	$^3A'$	$^3\Pi_{-1}$	$^3\Sigma$	$^3\Pi_{+1}$
B/ B_0	$\Delta E_{\text{exc}}/E_\text{h}$	$\Delta E_{\text{exc}}/E_\text{h}$	$\Delta E_{\text{exc}}/E_\text{h}$	$\Delta E_{\text{exc}}/E_\text{h}$	$\Delta E_{\text{exc}}/E_\text{h}$	$\Delta E_{\text{exc}}/E_\text{h}$
0.00	-1.681×10^{-3}	-2.701×10^{-4}	-1.681×10^{-3}	-1.681×10^{-3}	-2.701×10^{-4}	-1.681×10^{-3}
0.05	-9.882×10^{-4}	-1.650×10^{-3}	-1.225×10^{-3}	-2.833×10^{-3}	-1.382×10^{-3}	-2.834×10^{-3}
0.10	3.617×10^{-4}	-1.065×10^{-5}	2.545×10^{-5}	-7.222×10^{-3}	-5.809×10^{-3}	-7.223×10^{-3}
0.15	2.255×10^{-4}	9.926×10^{-5}	-2.964×10^{-5}	-1.006×10^{-2}	-8.712×10^{-3}	-1.006×10^{-2}
0.20	1.811×10^{-4}	1.793×10^{-4}	5.148×10^{-5}	-1.063×10^{-2}	-9.343×10^{-3}	-1.063×10^{-2}

Table S9: Shift in the transition wavelength and energies $\Delta\lambda = \lambda(\rho \to 0) - \lambda(\rho)$ ($\Delta E_{\text{exc}} = E_{\text{exc}}(\rho \to 0) - E_{\text{exc}}(\rho)$) on CD-CCSD ($\delta = 5$) level of the Mg triplet transition as a function of the helium density ρ of the $MgHe_{12}$ (C_{3h}) atmospheric model system in a magnetic field of 3000 T oriented along the C_3 axis. Employing the unc-aug-cc-pCVQZ on Mg and the unc-aug-cc-pVDZ basis on He.

n(He)/cm^{-3}	$B = 0$ $\Delta\lambda$/Å	$\Delta\lambda(E')$/Å	$B \neq 0$ $\Delta\lambda(A')$/Å	$\Delta E_{\text{exc}}(E')$/Å
1.94×10^{21}	6.23	4.70	5.38	6.25
4.12×10^{21}	100.62	81.60	93.31	108.26
6.55×10^{21}	305.95	254.96	290.91	336.78
1.13×10^{22}	760.85	649.64	737.79	849.94
2.21×10^{22}	1072.02	936.95	1065.32	1232.01
3.30×10^{22}	498.78	422.63	504.33	628.18
n(He)/cm^{-3}	$\Delta E_{\text{exc}}/E_{\text{h}}$	$\Delta E_{\text{exc}}(E')/E_{\text{h}}$	$\Delta E_{\text{exc}}(A')/E_{\text{h}}$	$\Delta E_{\text{exc}}(E')/E_{\text{h}}$
1.94×10^{21}	1.079×10^{-4}	9.468×10^{-5}	9.468×10^{-5}	9.483×10^{-5}
4.12×10^{21}	1.776×10^{-3}	1.672×10^{-3}	1.671×10^{-3}	1.674×10^{-3}
6.55×10^{21}	5.631×10^{-3}	5.424×10^{-3}	5.425×10^{-3}	5.439×10^{-3}
1.13×10^{22}	1.546×10^{-2}	1.515×10^{-2}	1.517×10^{-2}	1.525×10^{-2}
2.21×10^{22}	2.345×10^{-2}	2.349×10^{-2}	2.369×10^{-2}	2.409×10^{-2}
3.30×10^{22}	9.561×10^{-3}	9.338×10^{-3}	9.843×10^{-3}	1.075×10^{-2}

Table S10: Shift in the transition wavelength and energies $\Delta\lambda = \lambda(\rho \to 0) - \lambda(\rho)$ ($\Delta E_{\text{exc}} = E_{\text{exc}}(\rho \to 0) - E_{\text{exc}}(\rho)$) on CD-CCSD ($\delta = 5$) level of the Mg triplet transition as a function of the helium density ρ of the $MgHe_{12}$ (C_{3h}) atmospheric model system in a magnetic field of 30000 T oriented along the C_3 axis. Employing the unc-aug-cc-pCVQZ on Mg and the unc-aug-cc-pVDZ basis on He.

n(He)/cm^{-3}	$B = 0$ $\Delta\lambda$/Å	$\Delta\lambda(E')$/Å	$B \neq 0$ $\Delta\lambda(A')$/Å	$\Delta E_{\text{exc}}(E')$/Å
1.94×10^{21}	6.23	-0.45	-0.82	-5.76
4.12×10^{21}	100.62	-1.33	-2.49	-17.13
6.55×10^{21}	305.95	7.97	14.86	103.53
1.13×10^{22}	760.85	60.97	111.48	774.58
2.21×10^{22}	1072.02	182.98	324.98	2288.37
3.30×10^{22}	498.78	261.29	474.09	2404.29
n(He)/cm^{-3}	$\Delta E_{\text{exc}}/E_{\text{h}}$	$\Delta E_{\text{exc}}(E')/E_{\text{h}}$	$\Delta E_{\text{exc}}(A')/E_{\text{h}}$	$\Delta E_{\text{exc}}(E')/E_{\text{h}}$
1.94×10^{21}	1.079×10^{-4}	-3.073×10^{-5}	-2.949×10^{-5}	-3.059×10^{-5}
4.12×10^{21}	1.776×10^{-3}	-9.098×10^{-5}	-8.897×10^{-5}	-9.083×10^{-5}
6.55×10^{21}	5.631×10^{-3}	5.477×10^{-4}	5.338×10^{-4}	5.561×10^{-4}
1.13×10^{22}	1.546×10^{-2}	4.279×10^{-3}	4.117×10^{-3}	4.489×10^{-3}
2.21×10^{22}	2.345×10^{-2}	1.350×10^{-2}	1.279×10^{-2}	1.614×10^{-2}
3.30×10^{22}	9.561×10^{-3}	1.992×10^{-2}	1.956×10^{-2}	1.725×10^{-2}

Table S11: Transition wavelength and transition dipole moments $|\mu_{IJ}|^2$ on CD-CCSD ($\delta = 5$) level of the Mg triplet transition as a function of the helium density ρ of the $MgHe_{12}$ (C_{3h}) atmospheric model system in a magnetic field of 3000 T oriented along the C_3 axis. Employing the unc-aug-cc-pCVQZ on Mg and the unc-aug-cc-pVDZ basis on He.

$n(\text{He})/\text{cm}^{-3}$	$\Delta\lambda(E')/\text{Å}$	$\|\mu_{IJ}\|^2/e^2a_0^2$	$\Delta\lambda(A')/\text{Å}$	$\|\mu_{IJ}\|^2/e^2a_0^2$	$\Delta\lambda(E')/\text{Å}$	$\|\mu_{IJ}\|^2/e^2a_0^2$
1.94×10^{21}	4753.81	2.34	5086.34	2.37	5477.70	2.31
4.12×10^{21}	4676.90	2.37	4998.41	2.41	5375.69	2.36
6.55×10^{21}	4503.55	2.36	4800.81	2.39	5147.17	2.35
1.13×10^{22}	4108.86	2.07	4353.93	2.10	4634.01	2.09
2.21×10^{22}	3821.56	0.77	4026.41	0.80	4251.93	0.82
3.30×10^{22}	4335.88	0.00	4587.39	0.00	4855.77	0.05

Table S12: EOM-CC2 excitation energy of the $MgHe_{12}$ and $MgHe_{56}$ cluster using a lattice constant of 3 Å which equates to a density of 6.5×10^{21} atoms/cm^3. A magnetic field of 3000 T was oriented along the C_3 axis. The basis set on Mg was chosen to be unc-aug-cc-pCVQZ while the basis on He was unc-aug-cc-pVDZ.

		E'		A'		E'	
	$n(\text{He})/\text{cm}^{-3}$	$E_{\text{exc}}/E_\text{h}$	$\lambda/\text{Å}$	$E_{\text{exc}}/E_\text{h}$	$\lambda/\text{Å}$	$E_{\text{exc}}/E_\text{h}$	$\lambda/\text{Å}$
$MgHe_{12}$	6.5×10^{21}	0.101694	4482.82	0.094735	4812.14	0.090007	5064.90
$MgHe_{56}$	6.5×10^{21}	0.101820	4477.29	0.094861	4805.75	0.090132	5057.89
Difference			5.54		6.39		7.01

Table S13: Equilibrium geometries of the MgHe dimer in the triplet state as a function of the magnetic field strength.

	parallel	perpendicular
B/B_0	$R_{\text{eq}}/\text{Å}$	$R_{\text{eq}}/\text{Å}$
0	4.0744	4.0744
0.05	4.0961	6.2495
0.1	4.1414	5.3340
0.15	4.2000	4.6164
0.2	4.2677	4.0531

Table S14: Transition wavelength λ ($^3\Pi(^3A') \rightarrow ^3\Sigma^+(^3A')$ and $^3\Sigma^+(^3A'') \rightarrow {}^3\Sigma^+(A')$) as well as the total initial and final state energy E_{tot} as a function of the Mg-He distance R in a parallel and perpendicular magnetic field of 3000 T. Calculated at the CD-CCSD ($\delta = 5$) level using the unc-aug-cc-pCVQZ basis for Mg and the unc-aug-cc-pVDZ basis for He. The data is visualized in Fig. S6 and S7.

R/Å	$E_{\mathrm{tot}}(^3\Pi)/E_{\mathrm{h}}$	λ/Å	$E_{\mathrm{tot}}(^3\Sigma)/E_{\mathrm{h}}$	λ/Å	$E_{\mathrm{tot}}^{\mathrm{final}}(^3\Sigma)/E_{\mathrm{h}}$
2.5	-202.826805	4732.17	-202.797340	6817.37	-202.730470
3.0	-202.828475	4675.23	-202.811941	5629.83	-202.730966
3.5	-202.828911	4661.70	-202.818385	5224.00	-202.731119
4.0	-202.828967	4671.00	-202.821016	5085.29	-202.731370
4.5	-202.828940	4689.36	-202.822035	5047.88	-202.731725
5.0	-202.828907	4708.75	-202.822409	5047.54	-202.732092
5.5	-202.828885	4725.25	-202.822538	5057.99	-202.732408
6.0	-202.828873	4737.58	-202.822580	5069.11	-202.732647
6.5	-202.828866	4746.01	-202.822591	5077.75	-202.732811
7.0	-202.828862	4751.39	-202.822593	5083.59	-202.732916
7.5	-202.828860	4754.63	-202.822592	5087.23	-202.732980
8.0	-202.828859	4756.50	-202.822591	5089.36	-202.733016
8.5	-202.828858	4757.53	-202.822590	5090.55	-202.733036
9.0	-202.828858	4758.08	-202.822589	5091.19	-202.733047
9.5	-202.828857	4758.35	-202.822588	5091.51	-202.733052
10.0	-202.828857	4758.48	-202.822588	5091.66	-202.733054
R/Å	$E_{\mathrm{tot}}(^3A')/E_{\mathrm{h}}$	λ/Å	$E_{\mathrm{tot}}(^3A'')/E_{\mathrm{h}}$	λ/Å	$E_{\mathrm{tot}}^{\mathrm{final}}(^3A')/E_{\mathrm{h}}$
2.5	-202.821858	4995.41	-202.820610	5064.69	-202.730599
3.0	-202.825005	4855.57	-202.822181	5006.15	-202.731117
3.5	-202.827057	4759.41	-202.822634	4989.83	-202.731273
4.0	-202.828154	4716.48	-202.822696	4998.80	-202.731498
4.5	-202.828621	4709.67	-202.822669	5018.23	-202.731825
5.0	-202.828791	4718.12	-202.822637	5039.08	-202.732169
5.5	-202.828846	4729.92	-202.822615	5056.81	-202.732464
6.0	-202.828861	4740.11	-202.822603	5069.99	-202.732687
6.5	-202.828863	4747.46	-202.822597	5078.90	-202.732838
7.0	-202.828862	4752.22	-202.822593	5084.51	-202.732933
7.5	-202.828861	4755.10	-202.822591	5087.84	-202.732990
8.0	-202.828860	4756.75	-202.822590	5089.73	-202.733022
8.5	-202.828859	4757.65	-202.822589	5090.76	-202.733039
9.0	-202.828858	4758.13	-202.822588	5091.29	-202.733048
9.5	-202.828948	4753.91	-202.822588	5091.56	-202.733052
10.0	-202.828739	4761.76	-202.822698	5082.48	-202.733002

Table S15: Transition wavelength λ ($^3\Pi(^3A') \rightarrow ^3\Sigma^+(^3A')$ and $^3\Sigma^+(^3A'') \rightarrow {}^3\Sigma^+(A')$) as well as the total initial and final state energy E_{tot} as a function of the Mg-He distance R in a parallel and perpendicular magnetic field of 30 000 T. Calculated at the CD-CCSD ($\delta = 5$) level using the unc-aug-cc-pCVQZ basis for Mg and the unc-aug-cc-pVDZ basis for He. The data is visualized in Fig. S6 and S7.

R/Å	$E_{\mathrm{tot}}(^3\Pi)/E_{\mathrm{h}}$	λ/Å	$E_{\mathrm{tot}}(^3\Sigma)/E_{\mathrm{h}}$	λ/Å	$E_{\mathrm{tot}}^{\mathrm{final}}(^3\Sigma)/E_{\mathrm{h}}$
2.5	-202.947495	2343.97	-202.873824	3773.26	-202.753006
3.0	-202.949306	2345.80	-202.889685	3383.98	-202.754968
3.5	-202.949803	2393.12	-202.896516	3322.54	-202.759308
4.0	-202.949880	2444.26	-202.899241	3355.24	-202.763371
4.5	-202.949860	2491.57	-202.900268	3418.00	-202.766893
5.0	-202.949830	2530.75	-202.900627	3481.79	-202.769695
5.5	-202.949809	2559.00	-202.900738	3531.84	-202.771662
6.0	-202.949797	2575.64	-202.900764	3562.56	-202.772801
6.5	-202.949790	2582.69	-202.900764	3575.88	-202.773277
7.0	-202.949786	2583.86	-202.900759	3578.16	-202.773354
7.5	-202.949784	2582.67	-202.900755	3575.94	-202.773270
8.0	-202.949783	2581.23	-202.900752	3573.21	-202.773171
8.5	-202.949782	2580.25	-202.900751	3571.37	-202.773103
9.0	-202.949782	2579.75	-202.900750	3570.41	-202.773068
9.5	-202.949782	2579.52	-202.900749	3569.99	-202.773053
10.0	-202.949781	2579.43	-202.900749	3569.83	-202.773046
R/Å	$E_{\mathrm{tot}}(^3A')/E_{\mathrm{h}}$	λ/Å	$E_{\mathrm{tot}}(^3A'')/E_{\mathrm{h}}$	λ/Å	$E_{\mathrm{tot}}^{\mathrm{final}}(^3A')/E_{\mathrm{h}}$
2.5	-202.938595	2749.69	-202.899984	3584.45	-202.772803
3.0	-202.946127	2637.73	-202.900899	3572.69	-202.773298
3.5	-202.948867	2597.06	-202.900982	3571.27	-202.773331
4.0	-202.949652	2584.27	-202.900899	3571.25	-202.773247
4.5	-202.949815	2580.72	-202.900830	3570.98	-202.773168
5.0	-202.949824	2579.79	-202.900791	3570.52	-202.773113
5.5	-202.949809	2579.55	-202.900771	3570.21	-202.773082
6.0	-202.949797	2579.51	-202.900761	3570.07	-202.773067
6.5	-202.949791	2579.50	-202.900756	3570.01	-202.773060
7.0	-202.949787	2579.48	-202.900753	3569.95	-202.773055
7.5	-202.949785	2579.45	-202.900751	3569.88	-202.773051
8.0	-202.949783	2579.42	-202.900750	3569.82	-202.773047
8.5	-202.949783	2579.40	-202.900750	3569.78	-202.773045
9.0	-202.949782	2579.39	-202.900749	3569.74	-202.773044
9.5	-202.949782	2579.38	-202.900749	3569.73	-202.773043
10.0	-202.949781	2579.37	-202.900749	3569.72	-202.773042

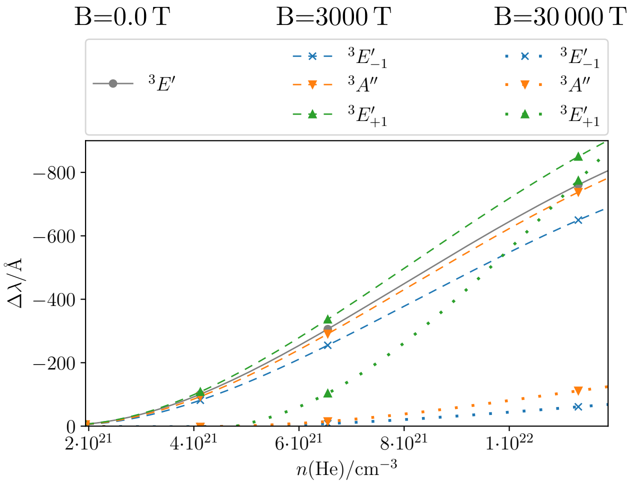

Figure S4: Shift in the transition wavelength $\Delta\lambda$ with respect atomic transition for triplet Mg as a function of the helium density ρ of the $MgHe_{12}$ (C_{3h}) atmospheric model system for the field-free case (grey full curve) and in a magnetic fields of 3000 T (dashed curves) as well as 30 000 T (dotted curves) oriented along the C_3 axis. Calculated at the CD-CCSD ($\delta = 5$) level employing the unc-aug-cc-pCVQZ on Mg and the unc-aug-cc-pVDZ basis on He.

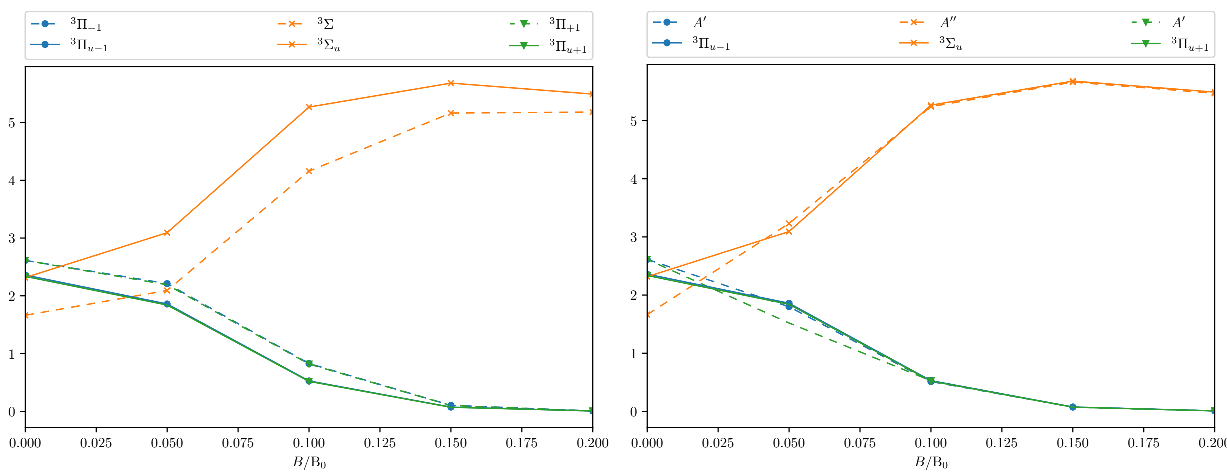

(a) parallel field

(b) perpendicular field

Figure S5: Evolution of the transition-dipole moment of the transitions in the triplet MgHe dimer as a function of the magnetic field strength (dashed lines). As reference the transition-dipole moment of an isolated atom is plotted (full lines). The calculations were performed using ff-CD-CCSD and the unc-aug-cc-pCVQZ basis for Mg and the unc-aug-cc-pVDZ basis for He.

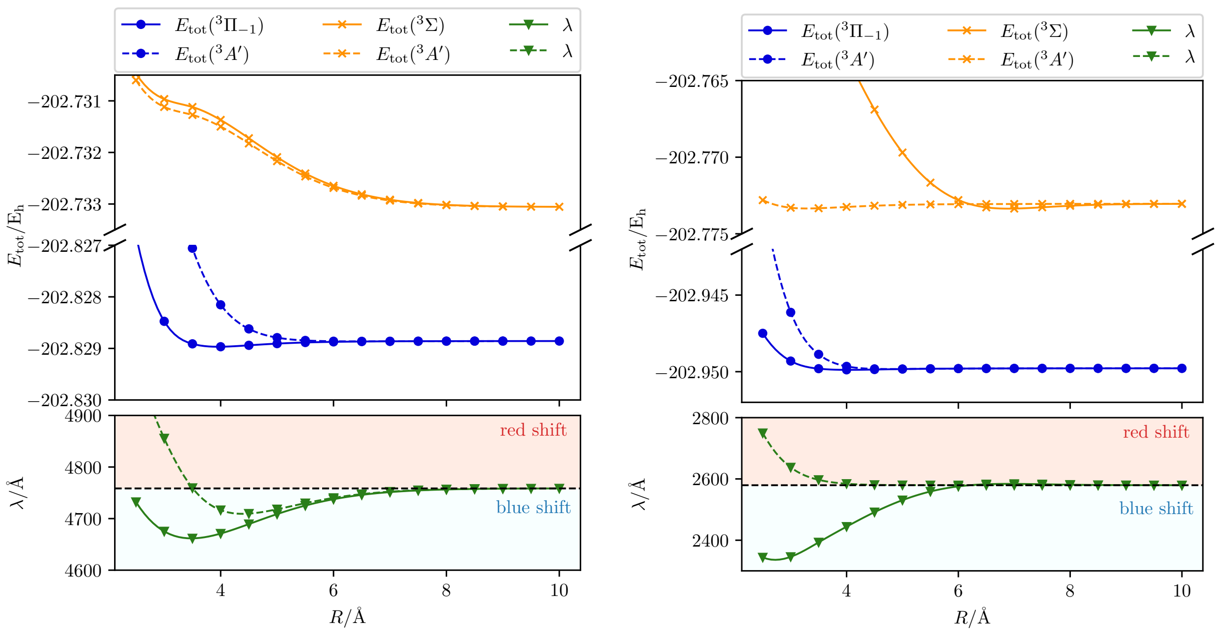

(a) 3000 T (b) 30000 T

Figure S6: Transition wavelengths λ in a parallel ($^3\Pi_{-1} \rightarrow {}^3\Sigma$, full lines) and perpendicular orientation ($^3A' \rightarrow {}^3A'$, dashed lines) in a magnetic field of 3000 T and 30000 T as well as the total initial-state energy E_{tot} as a function of the Mg-He distance R. Calculated with CD-CCSD (δ = 5) using the unc-aug-cc-pCVQZ basis for Mg and the unc-aug-cc-pVDZ basis for He.

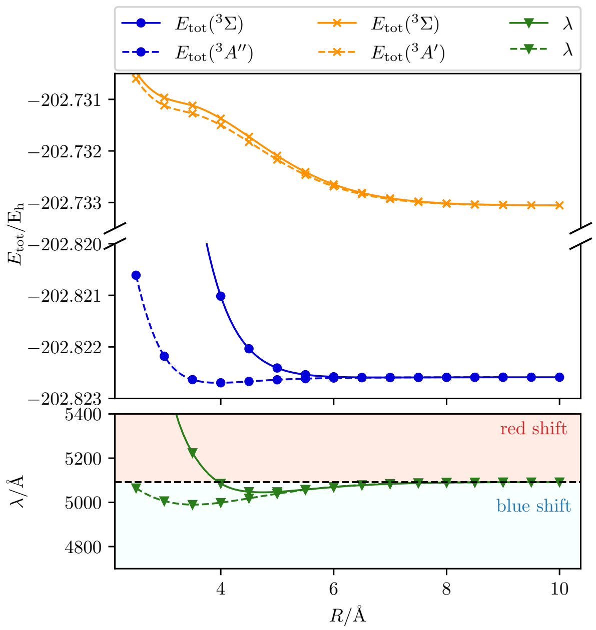

(a) 3000 T

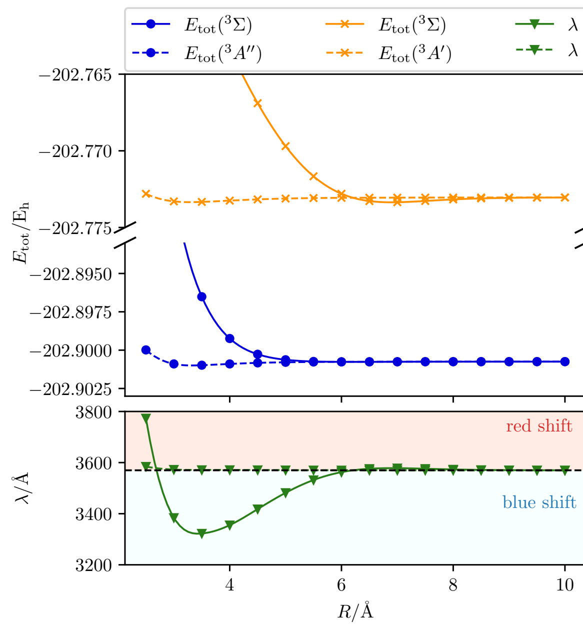

(b) 30000 T

Figure S7: Transition wavelengths λ in a parallel ($^3\Sigma \rightarrow {}^3\Sigma$, full lines) and perpendicular orientation ($^3A'' \rightarrow {}^3A'$, dashed lines) in a magnetic field of 3000 T and 30000 T as well as the total initial-state energy E_{tot} as a function of the Mg-He distance R. Calculated with CD-CCSD ($\delta = 5$) using the unc-aug-cc-pCVQZ basis for Mg and the unc-aug-cc-pVDZ basis for He.